

# Lithography at a wavelength of 193 nm

by M. Rothschild  
A. R. Forte  
R. R. Kunz  
S. C. Palmateer  
J. H. C. Sedlacek

**The trend in microelectronics toward printing features 0.25  $\mu\text{m}$  and below has motivated the development of lithography at the 193-nm wavelength of argon fluoride excimer lasers. This technology is in its early stages, but a picture is emerging of its strengths and limitations. The change in wavelength from 248 to 193 nm requires parallel progress in projection systems, optical materials, and photoresist chemistries and processes. This paper reviews the current status of these various topics, as they have been engineered under a multiyear program at MIT Lincoln Laboratory.**

## Introduction

The relentless drive in the integrated circuit industry toward greater packing density and higher speeds has served as the impetus for optical lithography to reduce printed image sizes from 2  $\mu\text{m}$  twenty years ago to less than 0.5  $\mu\text{m}$  today. This remarkable progress has been made possible by improved lens quality, increases in numerical aperture, improved resist processes, and the use of increasingly shorter exposure wavelengths. Today's photolithography uses wavelengths of 365 or 248 nm for imaging the smallest possible feature sizes, thus employing aggressively low lithographic  $k_1$  factors of 0.5 to 0.6. However, as image dimension requirements drop below 0.25  $\mu\text{m}$  in the next few years, it will be necessary to consider even shorter exposure wavelengths. An obvious candidate for extension to shorter wavelengths is the 193-nm laser line produced by the argon fluoride (ArF)

excimer laser. Indeed, the recent Semiconductor Industry Association roadmap lists 193 nm as one of the options for printing 0.18  $\mu\text{m}$ , along with extensions of 248 nm. While each of the alternatives has its own advantages and risks, only those of 193 nm are discussed here.

The change to 193 nm poses challenges and opens up new possibilities, as new photoinduced processes take place at this shorter wavelength. Specifically, optical materials that are nominally transparent have weak absorption and also undergo laser-induced changes, and few organic polymers are transparent enough to serve as single-layer resists. On the other hand, efficient photoinduced cross-linking of polymers or oxidation of silicon-containing polymers may enable new near-surface resist processes.

This paper reviews the progress that has been made at MIT Lincoln Laboratory toward a production-worthy 193-nm technology at sub-0.25- $\mu\text{m}$  resolution [1]. The Lincoln Laboratory program has addressed in parallel both the construction of a full-field prototype exposure system (including the evaluation of optical materials and coatings) and the development of photoresist processes (single layer, antireflective layer, top-surface imaging, bilayers, and all-dry resists).

## Projection system

A full-field prototype 193-nm step-and-scan exposure system was built by SVG Lithography (SVGL), and it was installed in Lincoln Laboratory's clean room at the end of 1993. This system is the world's first—and at present the only—large-field 193-nm prototype exposure tool. It has a 193-nm 0.50-numerical aperture (NA) lithographic lens with 4 $\times$  demagnification, mounted on a commercial SVGL

©Copyright 1997 by International Business Machines Corporation. Copying in printed form for private use is permitted without payment of royalty provided that (1) each reproduction is done without alteration and (2) the Journal reference and IBM copyright notice are included on the first page. The title and abstract, but no other portions, of this paper may be copied or distributed royalty free without further permission by computer-based and other information-service systems. Permission to *republish* any other portion of this paper must be obtained from the Editor.

Micrascan® II body. The slit size is  $22 \times 5$  mm, and the fully scanned field is  $22 \times 32.5$  mm. In addition to its large field, a distinctive feature of this tool is its off-axis alignment subsystem. It provides an overlay accuracy of better than 40 nm ( $3\sigma$ ), thus enabling the fabrication of devices by all-193-nm lithography. A mix-and-match process involving other tools for noncritical levels also requires distortion matching. The dynamic distortion in this system has been measured, and the largest vectors are 77 nm over the full field.

The 193-nm Micrascan uses a catadioptric lens design incorporating both reflective and refractive optical elements. The chromatic aberration of this design is low enough to accommodate the natural 0.5-nm excimer laser bandwidth [2]. This is in sharp contrast to all-refractive deep-UV (248-nm) lithographic lenses, which typically require special modifications to the laser to deliver an optical bandwidth of less than 0.001 nm FWHM. The ability of the catadioptric lens to use the natural bandwidth of the ArF laser considerably eases the demands on the laser design.

The projection optics consist of an aspheric concave mirror used as a  $4\times$  reduction lens, with a cube beam splitter between the mirror and the water surface. Several refractive optical elements are included in the design for aberration control. All refractive elements, including the cube beam splitter, are made of a selected grade of fused silica. The cube beam splitter, which contains the greatest part of the optical path length in fused silica, was tested extensively for transparency at 193 nm before fabrication, and had a bulk absorption of  $\sim 0.4\%$  per centimeter. The optical transmission of the 193-nm projection optics is approximately half that of the equivalent 248-nm optics.

The laser in the 193-nm Micrascan was built by Cymer Laser. It is able to produce its designed 6-W average power (linearly polarized) at 350 Hz with new optical elements. As the laser ages, the power level characteristically drops, owing to increased levels of damage in bulk optical materials and coatings within the laser. Replacement of damaged optical elements essentially restores the laser to its original power level. Typical lifetimes of optical components within the laser range from several weeks to several months, with large variations among materials from different sources.

### Optical materials

In parallel with the construction of the 193-nm Micrascan, we have been studying the performance of optical materials at 193 nm. Few optical materials are transparent enough at 193 nm to enable the fabrication of a high-quality all-refractive or catadioptric system as required for a lithographic lens. High-purity synthetic fused silica and crystalline calcium fluoride are probably the only practical choices [3], with fused silica having the edge for reasons

of cost and existing processing infrastructure. For purposes of insertion into 193-nm lithography, the ideal optical material should be fully transparent, and should remain unchanged after several billions of pulses. In practice, fused silica has an absorption coefficient of 0.005 to  $0.10 \text{ cm}^{-1}$  with large variations from grade to grade and even from sample to sample. Since the temperature coefficient of the index of refraction of fused silica at 193 nm is  $\sim 2 \times 10^{-5} \text{ }^\circ\text{C}^{-1}$ , the magnitude of the allowable absorption coefficient is determined by system considerations, including laser power and the specific design of the projection optics. A value of  $0.10 \text{ cm}^{-1}$  is clearly unacceptable, but the range 0.001 to  $0.01 \text{ cm}^{-1}$  requires careful analysis with respect to each system design. It should be noted that the physical origin of the absorption at 193 nm is not yet clearly understood. With metallic impurities reduced to the sub-ppm level, the main candidates are Cl impurities (residue from the starting material  $\text{SiCl}_4$ ), hydroxyl (OH) impurities, and imperfect stoichiometry, i.e., excess oxygen or oxygen deficiency [4]. Similar considerations apply to scattering losses, the most important one being Rayleigh scattering caused by density fluctuations. The fundamental lower limit for this process at 193 nm may be in the range  $10^{-3}$ – $10^{-4} \text{ cm}^{-1}$  [5].

Beyond the amount of initial absorption and scattering, the optical material should be resistant to radiation-induced changes ("damage") over the practical lifetime of a projection system. The principal modes of laser-induced damage in fused silica are color center formation and optical compaction [6]. The color centers are E' centers, consisting of an unpaired electron on a silicon atom, accompanied by oxygen vacancy. Formation of E' color centers leads to absorption at  $\sim 215$  nm, with increased optical absorption also at 193 nm. Compaction manifests itself as reduced thickness accompanied by an increased index of refraction [6, 7]. The net result is a decrease in the optical path, which in a lithographic lens would cause wavefront aberrations and loss of image quality. The two types of damage seem to depend on different properties of the fused silica; a sample with good resistance to color center formation does not necessarily have good resistance to compaction. Typical samples seem to be more sensitive to compaction than to color center formation. Furthermore, recent samples of fused silica exhibit saturationlike behavior of the color centers, with laser-induced absorption coefficients saturating at  $\sim 0.001 \text{ cm}^{-1}$ , for  $1\text{--}5 \text{ mJ/cm}^2/\text{pulse}$ . This added value is less than the initial absorption coefficient, or  $\sim 0.002 \text{ cm}^{-1}$ . Thus, it is expected that compaction, and not color centers, sets the limit on allowable power densities within the lithographic lens.

At low values of compaction in fused silica, the compaction increases linearly with the number of pulses and as the square of the peak intensity  $I$  within a laser

pulse. This behavior is the signature of a two-photon process, whose coefficient  $\alpha_1 = \beta I$  is linear in  $I$ . (The compaction, being proportional to the product of  $I$  and  $\alpha_1$ , behaves as  $I^2$ .) The coefficient  $\beta$  is intrinsic to the material, and has been measured to be  $\sim 2 \times 10^{-3}$  to  $2 \times 10^{-4}$  cm/MW [8, 9]. Because excimer laser pulses are extremely short (typically between 5 and 20 ns FWHM), high peak intensities are generated by pulse trains of modest average intensities. Consequently,  $\alpha_1$  may be non-negligible. For instance, at a fluence of 10 mJ/cm<sup>2</sup> and pulse duration of 20 ns,  $I = 0.5$  MW/cm<sup>2</sup>, and  $\alpha_1 \approx 10^{-3}$ – $10^{-4}$  cm<sup>-1</sup>. Estimates have been made that a 10-year lifetime of a 193-nm fused silica lithographic lens can be achieved with the best existing grades of fused silica if the energy density per pulse is kept at or below 1 mJ/cm<sup>2</sup> within any element of the lens. This restriction forces the use of relatively sensitive photoresists; dose requirements of 25 mJ/cm<sup>2</sup> or less would be needed to achieve a 50-wafer-per-hour throughput on 8-inch wafers. Higher-dose resists could be accommodated with future advances in damage resistance of fused silica or possibly with substitution of CaF<sub>2</sub> in critical elements of the lens.

Calcium fluoride (CaF<sub>2</sub>) does not suffer from compaction because of the crystalline nature of the material. It is susceptible to color center formation, but this susceptibility is apparently due only to defects and impurities in the material. Current high-purity CaF<sub>2</sub> is significantly better than that available a decade ago. In fact, it is comparable to or better than fused silica in its resistance to damage [10]. The main technical barriers against extensive use of calcium fluoride as a 193-nm lens material are residual stress birefringence and lack of experience with its grinding and polishing characteristics.

It should be noted that the results discussed above have been obtained from experiments performed off-line. To date, there is no evidence that the Micrascan optics have suffered the kind of bulk damage seen on samples at higher fluences.

The properties of bulk optical materials are but one item in the list of optics-related topics that have to be addressed at 193 nm. Others include the behavior of dielectric coatings [3], pellicles [11], and photoinduced organic deposits on surfaces. These are also the subject of ongoing studies at Lincoln Laboratory.

### Photoresists

The most difficult challenge in bringing 193-nm lithography to full manufacturing use may be the development of a robust photoresist process. The resins which are typically used for I-line (365-nm) and 248-nm photoresists, e.g., novolac and poly(hydroxystyrene), have absorption depths of 30 to 50 nm at 193 nm, and therefore are far too opaque to be used in single-layer resists at that wavelength. Since methacrylates are

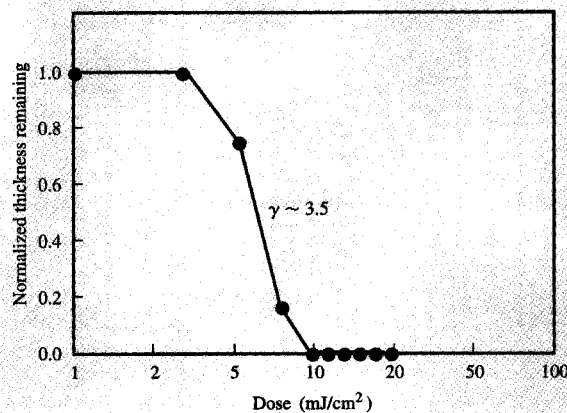


**Figure 1**

Contrast curve for poly(MMA-co-tBMA-co-MAA) with 1% bis(*t*-butylphenyl) iodonium triflate, developed in 0.01-N TMAH after a 130°C, 1-minute post-exposure bake. The contrast  $\gamma$  is  $\sim 3.5$ . © Copyright IEEE [*IEEE J. Select. Topics Quantum Electron.* 1, 916 (1995)].

semitransparent at 193 nm, these polymers can serve as the basis for 193-nm single-layer resists. Acid-catalyzed conversion of *t*-butyl methacrylate (tBMA) into methacrylic acid (MAA) provides the chemical underpinning for several versions of such resists, developed under a collaboration between MIT Lincoln Laboratory and the IBM Almaden Research Center [12, 13].

These systems contain resins synthesized by free-radical solution terpolymerization of tBMA (fraction  $x$ ), methylmethacrylate (MMA, fraction  $y$ ), and MAA (fraction  $z$ ), and meet the transparency and thermal stability requirements for single-layer resist applications. A typical composition has  $x/y/z \approx 0.4/0.4/0.2$ , and the glass transition temperature ( $T_g$ ) is in the range 140–160°C. The absorption coefficient of these base resins at 193 nm is around  $0.08 \mu\text{m}^{-1}$ . **Figure 1** shows the contrast curve of a two-component resist including such a terpolymer and a photoacid generator.

The solubility of these terpolymers can be controlled by variations in MAA content. For example, when the MAA concentration is  $\sim 20$  mole percent, the exposed films are aqueous-base-soluble only after exposure, whereas at MAA fractions approaching 30 mole percent, the unexposed resin itself becomes aqueous-base-soluble.

Since they are photosensitive also at 248 nm, the methacrylate-based resists have the added advantage that they can serve as effective dual-wavelength resists. Indeed, the dual-wavelength property has enabled their

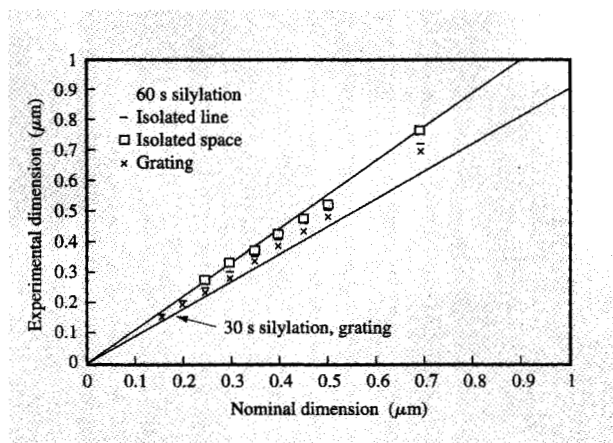


**Figure 2**

Silylation process linearity at best dose. A 0.76- $\mu\text{m}$ -thick poly(vinylphenol) resist was silylated with dimethylsilyldimethylamine at 90°C and 25 torr for 60 s, and then was etched under optimized conditions with a 100% over-etch. With 30 s silylation and 25% over-etch the linearity for gratings covers the 0.175–0.70- $\mu\text{m}$  range, but linearity for isolated features is not obtained below 0.2  $\mu\text{m}$ . The two solid lines are the acceptable performance, i.e.,  $\pm 10\%$  deviations from the nominal feature size. ©Copyright IEEE [IEEE J. Select. Topics Quantum Electron. 1, 916 (1995)].

development at 248 nm, while the 193 Micrascan has been undergoing its own tests and modifications.

The main drawback of these photoresists is their low etch resistance in subsequent plasma processing steps, especially in the chlorine-based chemistries required for metal etching. Increased etch resistance can be obtained by incorporation of high-carbon-content polymers. These cannot be aromatics because of limitations of transparency. The alternative is copolymerization with polymers containing pendant alicyclics, such as adamantyl methacrylates [14]. Resultant tetrapolymers have been synthesized and have been shown to have significantly lower etch rates, 1.4 $\times$  that of novolac, compared to 2.2 $\times$  that of novolac for the terpolymers. Another option under study for increasing etch resistance involves the development of three component systems (including the addition of dissolution inhibitors which, because of their high carbon-to-hydrogen ratio, also reduce the plasma etch rate of the resist system).

Top-surface-imaged (TSI) resists have been developed at longer wavelengths as an alternative to bulk-imaged resists [15]. Their main potential advantages are a larger depth of focus, especially for sub-0.25- $\mu\text{m}$  lithography, where the thickness of single-layer resists becomes comparable to the theoretical optical depth of focus, and the elimination of the need for antireflective layers. TSI processes operate via area-selective in-diffusion of a silyl

amine into a phenolic polymer to form a silyl ether. Once the silicon has been selectively incorporated, the latent image is developed in an anisotropic oxygen plasma etch. At 193 nm, the simplest TSI resist scheme is a positive-tone process, based on photo-cross-linking of the single component poly(vinylphenol) (PVP), followed by selective silylation of the unexposed areas and plasma etching [16].

The silylation is performed with dimethylsilyldimethylamine (DMSDMA), at a temperature of 90°C and a pressure of 25 torr for 30 to 75 s. The un-cross-linked PVP areas incorporate a controlled amount of silicon, whereas the cross-linked areas do not. The wafers are then dry-developed in a high-ion-density helicon etcher in an oxygen-based plasma. The oxygen reacts with the silylated areas to form  $\text{SiO}_2$ , which acts as an etch mask in the unexposed areas.

On the basis of initial materials characterization, we chose to use DMSDMA to silylate PVP because of its high vapor pressure and small molar volume, which allows it to diffuse rapidly at low temperatures. This is useful for our high-molecular-weight PVP resist, which has a higher  $T_g$ ,  $\sim 180^\circ\text{C}$ , than many multiple-component chemically amplified TSI resists. One effect of this high  $T_g$  is slower diffusion rates, which can be minimized by going to lower-molar-volume silylating agents.

The overall lithographic performance of the silylation process depends on both the silylation step (i.e., the silylation mask shape) and the dry-development step (i.e., selectivity, vertical/lateral etch rates, and amount of over-etch). Figure 2 demonstrates the excellent linearity obtained with the 0.5-NA 193-nm Micrascan and the TSI process outlined above. For a wafer temperature in the helicon etcher of  $-70^\circ\text{C}$ , linearity is maintained down to 0.20  $\mu\text{m}$  for both 25% and 100% over-etch. For an etch temperature of 30°C, linearity is maintained down to 0.20  $\mu\text{m}$  for a 25% over-etch, but only to 0.30  $\mu\text{m}$  for a 100% over-etch. This is due to an increased isotropic etching component at 30°C. The grating-to-isolated-line bias for a 60-s silylation time decreases from 30 nm for the 25% over-etch, to 5 nm for the 100% over-etch. The linearity of gratings, but not of isolated lines, was extended down to 0.175  $\mu\text{m}$  by reducing the silylation time from 60 to 30 s.

Figure 3 is a graphic representation of the exposure-dose matrix for 0.25-, 0.20-, and 0.175- $\mu\text{m}$  gratings for a 30-s silylation time and a 25% over-etch. At best dose the depth of focus is 1.6, 1.0, and 1.0  $\mu\text{m}$ , respectively. However, this maximum depth of focus is obtained at higher doses as the feature size decreases. Such behavior is in qualitative agreement with aerial image simulations and corresponding exposure-defocus plots. The simulation predicts an 8.5% increase in best dose when the grating lines are reduced from 0.25 to 0.20  $\mu\text{m}$ . This result is in close agreement with the 10% dose increase measured

experimentally. It should be noted that the data tabulated above are based on printed features which have near-vertical sidewalls. **Figure 4** shows representative SEMs of 0.20-, 0.175-, and 0.15- $\mu\text{m}$  resist features obtained as described above.

### Conclusions

Fundamental optics principles have motivated the trend in photolithography toward shorter wavelengths. One of the main alternatives in the printing of 0.18- $\mu\text{m}$  devices, whose mass production is expected to start around the year 2001, is lithography at the 193-nm wavelength of ArF excimer lasers. The transition from 248 to 193 nm is viewed as largely evolutionary, following the trend from 436 to 365 to 248 nm. Nevertheless, new infrastructures must be developed, mainly in the areas of optical materials and photoresists. Under the MIT Lincoln Laboratory program, a full-field 193-nm prototype step-and-scan system has been built and is currently undergoing tests and modifications of its subsystems. Bulk optical materials and coatings are continuously being tested for absorption and resistance to laser-induced damage. First-generation single-layer resist systems (including antireflective layers [17]) and TSI processes have been developed. Initial experimental results indicate that key requirements of such resists, such as 0.18- $\mu\text{m}$  resolution and 1- $\mu\text{m}$  depth of focus, can indeed be met. Other resist schemes have also been demonstrated, although they are technically less mature than TSI and therefore have not been detailed in this paper. These include bilayer resists with polysilyne imaging layers [18] and plasma-deposited, plasma-developed counterparts of bilayers and of TSI ("all-dry resists") [19, 20]. However, significant additional work is required in order to transform the current proof-of-concept demonstrations into a robust manufacturing technology. Critical associated technologies must be developed and tested as well. These include overlay, metrology, and mask writing—all at the dimensions dictated by the insertion point of the 0.18- $\mu\text{m}$  critical dimension. Some of these technologies, such as overlay, are not specific to the 193-nm actinic wavelength, while others, such as materials for attenuating phase shifting masks, are. They must all be brought to a significant level of maturity at an accelerated pace to permit insertion into pilot lines within the next three years.

### Acknowledgments

The work on single-layer resists was performed under a collaboration with the IBM Almaden Research Center, mainly with R. D. Allen, R. A. DiPietro, D. C. Hofer, and G. M. Wallraff. We thank M. Hibbs (IBM Essex Junction) who, as a Sematech assignee at Lincoln Laboratory, worked closely with us in the evaluation of the performance of the 193-nm Micrascan. We also thank

Gratings ( $\mu\text{m}$ )	$k_1$ factor	Defocus ( $\mu\text{m}$ )	Dose ( $\text{mJ}/\text{cm}^2$ )						Exposure latitude (%)
			100	110	121	133	146	161	
0.250	0.65	1.2							30
		1.0							
		0.8							
		0.6	0.8						
		0.4	1.6						
		0.2		0.4		0.2			
		0							
0.200	0.52	0.8						20	
		0.6							
		0.4							
		0.2	0.2		1.0	1.0			
		0							
		-0.2							
		-0.4							
0.175	0.42	0.6						20	
		0.4							
		0.2							
		0							
		-0.2			0.2	1.0	0.6		
		-0.4							

**Figure 3**

Experimental exposure-dose matrix for 0.25- $\mu\text{m}$ , 0.20- $\mu\text{m}$ , and 0.175- $\mu\text{m}$  gratings ( $\pm 10\%$  of critical dimension). A 0.50- $\mu\text{m}$ -thick PVP resist was silylated with DMSDMA at 90°C and 25 torr for 30 s, and then was etched under optimized conditions with a 25% over-etch. ©Copyright IEEE [*IEEE J. Select. Topics Quantum Electron.* 1, 916 (1995)].

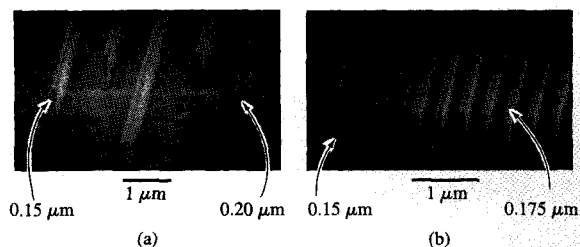


**Figure 4**

Scanning electron micrographs of (a) 0.15- $\mu\text{m}$ , 0.175- $\mu\text{m}$ , and 0.2- $\mu\text{m}$  isolated lines and (b) 0.15- $\mu\text{m}$  and 0.175- $\mu\text{m}$  dense features printed with 193-nm top-surface imaging. The doses in (a) and (b) were not the same. ©Copyright IEEE [*IEEE J. Select. Topics Quantum Electron.* 1, 916 (1995)].

M. W. Horn for helpful discussions, and D. Downs, L. Eriksen, and C. Marchi for their technical assistance. This work was sponsored by the Defense Advanced Research Projects Agency's Advanced Lithography Program.

Opinions, interpretations, conclusions, and recommendations are those of the authors and are not necessarily endorsed by the United States Air Force.

Micrascan is a registered trademark of SVG Lithography Systems, Inc.

## References

1. For earlier reviews, see (a) M. Rothschild, R. B. Goodman, M. A. Hartney, M. W. Horn, R. R. Kunz, J. H. C. Sedlacek, and D. C. Shaver, "Photolithography at 193 nm," *J. Vac. Sci. Technol. B* **10**, 2989 (1992); (b) M. Hibbs, R. R. Kunz, and M. Rothschild, "193-nm Lithography at MIT Lincoln Lab," *Solid State Technol.* **38**, No. 7, 69 (1995).
2. R. Sandstrom, "Argon Fluoride Excimer Laser Source for Sub-0.25- $\mu\text{m}$  Optical Lithography," *Proc. SPIE* **1463**, 610-616 (1991).
3. M. Rothschild, "Optical Materials for Excimer Laser Applications," *Opt. Photon. News* **4**, No. 5, 8 (1993).
4. K. Awazu and H. Kawazoe, " $\text{O}_2$  Molecules Dissolved in Synthetic Silica Glasses and Their Photochemical Reactions Induced by ArF Excimer Laser Radiation," *J. Appl. Phys.* **68**, 3584 (1990).
5. M. E. Lines, J. B. MacChesney, K. B. Lyons, A. J. Bruce, A. E. Miller, and K. Nassou, "Calcium Aluminate Glasses as Potential Ultralow-Loss Optical Materials at 1.5-1.9  $\mu\text{m}$ ," *J. Non-Cryst. Solids* **107**, 251 (1989).
6. M. Rothschild and J. H. C. Sedlacek, "Excimer Laser Degradation in Bulk Fused Silica," *Proc. SPIE* **1848**, 537 (1992).
7. R. Schenker, P. Schermerhorn, and W. G. Oldham, "Deep-Ultraviolet Damage to Fused Silica," *J. Vac. Sci. Technol. B* **12**, 3275 (1994).
8. R. S. Taylor, K. E. Leopold, R. K. Brimacombe, and S. Mihailov, "Dependence of the Damage and Transmission Properties of Fused Silica Fibers on the Excimer Laser Wavelength," *Appl. Opt.* **27**, 3124-3134 (1988).
9. O. Kittelman and J. Ringling, "Intensity-Dependent Transmission Properties of Window Materials at 193-nm Irradiation," *Opt. Lett.* **19**, 2053 (1994).
10. J. H. C. Sedlacek and M. Rothschild, "Optical Materials for Use with Excimer Lasers," *Proc. SPIE* **1835**, 80 (1992).
11. M. Rothschild and J. H. C. Sedlacek, "Laser Induced Damage in Pellicles at 193 nm," *Proc. SPIE* **1674**, 618 (1992).
12. R. D. Allen, G. M. Wallraff, W. D. Hinsberg, and L. L. Simpson, "High Performance Acrylic Polymers for Chemically Amplified Photoresist Applications," *J. Vac. Sci. Technol. B* **9**, 3357-3361 (1991).
13. R. R. Kunz, R. D. Allen, W. D. Hinsberg, and G. M. Wallraff, "Acid-Catalyzed Single-Layer Resists for ArF Lithography," *Proc. SPIE* **1925**, 167 (1993).
14. R. D. Allen, G. M. Wallraff, R. A. DiPietro, D. C. Hofer, and R. R. Kunz, "Design Considerations for 193 nm Positive Resists," *Proc. Amer. Chem. Soc. Natl. Symp.* **72**, 100 (1995).
15. T. M. Wolf, G. N. Taylor, T. Venkatesan, and R. R. Kraetsch, "The Scope and Mechanism of New Positive Tone Gas Phase Functionalized Plasma Developed Resists," *J. Electrochem. Soc.* **131**, 1664-1670 (1984).
16. M. A. Hartney, M. Rothschild, R. R. Kunz, D. J. Ehrlich, and D. C. Shaver, "Silylation Processes Based on Ultraviolet Laser-Induced Crosslinking," *J. Vac. Sci. Technol. B* **8**, 1476 (1990).
17. R. R. Kunz and R. D. Allen, "Materials Evaluation of Antireflective Coatings for Single-Layer 193-nm Lithography," *Proc. SPIE* **2195**, 447 (1994).
18. R. R. Kunz, M. W. Horn, P. A. Bianconi, D. A. Smith, and J. R. Eschelman, "Wet-Developed Bilayer Resists for 193-nm Excimer Laser Lithography," *J. Vac. Sci. Technol. B* **10**, 2554 (1992).
19. M. W. Horn, S. W. Pang, and M. Rothschild, "Plasma-Deposited Organosilicon Thin Films as Dry Resists for Deep Ultraviolet Lithography," *J. Vac. Sci. Technol. B* **8**, 1493 (1990).
20. M. W. Horn, B. E. Maxwell, R. R. Kunz, M. S. Hibbs, L. M. Eriksen, S. C. Palmateer, and A. R. Forte, "All-Dry Resist Processes for 193-nm Lithography," *Proc. SPIE* **2438**, 760 (1995).

Received February 9, 1996; accepted for publication September 14, 1996

**Mordechai Rothschild** *Lincoln Laboratory, Massachusetts Institute of Technology, Lexington, Massachusetts 02173 (rothschild@ll.mit.edu)*. Dr. Rothschild received his Ph.D. in 1979 in optics from the University of Rochester. Following research at the University of Illinois and the University of Southern California in the areas of laser photochemistry and laser-induced nonlinear processes, in 1984 he joined MIT Lincoln Laboratory, where he is currently leader of the Submicrometer Technology Group. His responsibilities include managing the advanced lithography projects at Lincoln Laboratory, as well as binary optics and several other microfabrication activities.

**Anthony R. Forte** *Lincoln Laboratory, Massachusetts Institute of Technology, Lexington, Massachusetts 02173*. Mr. Forte received an associate's degree in computer engineering from Franklin Institute, Boston, in 1980. In the same year, he began working at MIT Lincoln Laboratory with the Microelectronics Group, working primarily toward the development of dry etching of metals. Additional responsibilities included the development of noncrystallographic dry-etch processes for GaAs, as well as high-aspect-ratio dry-etching of silicon for permeable-base transistors. In 1988 Mr. Forte joined the Submicrometer Technology Group at MIT Lincoln Laboratory, developing plasma-deposited electrochromic thin films for use in 193-nm lithography. Currently he is developing silylation processes for top-surface imaging and the corresponding dry-etch processes for pattern transfer for 193-nm lithography.

**Roderick R. Kunz** *Lincoln Laboratory, Massachusetts Institute of Technology, Lexington, Massachusetts 02173*. Dr. Kunz received his B.S. in chemistry from Rensselaer Polytechnic Institute in 1983 and his Ph.D. in chemistry from the University of North Carolina at Chapel Hill in 1988, working at the IBM Thomas J. Watson Research Center in 1987. Since 1988, he has been a staff member in the Submicrometer Technology Group at MIT Lincoln Laboratory, where his principal focus has been the development of 193-nm photoresist processes and the investigation of excimer laser direct processes such as deposition and *in situ* patterning. Prior to joining Lincoln Laboratory, Dr. Kunz studied the fundamental aspects of both particle-beam-induced and etch processes.

**Susan C. Palmateer** *Lincoln Laboratory, Massachusetts Institute of Technology, Lexington, Massachusetts 02173*. Dr. Palmateer received the B.S. degree in chemistry from Monmouth College, West Long Branch, New Jersey, in 1979, and the M.S. and Ph.D. degrees from Cornell University in 1982 and 1985, in electrical engineering and electrophysics, respectively. In November 1985, she became a staff member in the Electrooptical Devices Group at MIT Lincoln Laboratory. Dr. Palmateer was responsible for the development of organometallic chemical vapor deposition and gas source molecular beam epitaxy for the growth of gallium-, indium-, and aluminum-containing arsenides and phosphides for optical and electronic applications. In June 1993 she joined the Submicrometer Technology Group at Lincoln Laboratory and is developing top-surface imaging for 193-nm lithography.

**Jan H. C. Sedlacek** *Lincoln Laboratory, Massachusetts Institute of Technology, Lexington, Massachusetts 02173*. Mr. Sedlacek received a B.A. in physics from Reed College, Portland, Oregon, in 1976. After joining Lincoln Laboratory in April 1982, he worked on laser photochemistry for laser direct-write processing. For the past five years he has been involved in studies of optical materials for 193-nm lithography. Mr. Sedlacek is a member of the AAAS and SPIE.